

IMAGES FROM LARGE SCHMIDT TELESCOPES

D.S. Brown

Grubb Parsons Ltd., Walkergate, Newcastle upon Tyne, U.K.

C.N. Dunlop and J.V. Major

Department of Physics, The University, Durham, U.K.

ABSTRACT: Calculations have been made of the intensity distribution of star images formed at the focal surface of large Schmidt telescopes. The calculations take account of atmospheric seeing, aperture diffraction, manufacturing errors, chromatic errors in the corrector plate, scattering in the emulsion, photographic response and grain structure. The results are expressed in terms of simulated microdensitometer scans across the processed emulsion.

Results are given for a system S1(1.24m, $f/2.5$) similar to the 48" U.K. Schmidt (with both singlet and achromat corrector plates) for several combinations of correctors and filters using IIIa-J emulsion for recording. The improvement in performance expected from the use of larger Schmidt telescopes is discussed and results are given for two designs with 2.5 metres aperture, S2(2.5m, $f/2.5$) and S3(2.5m, $f/3$).

1. INTRODUCTION

In a typical, large Schmidt starlight from an aperture > 1 metre is focussed at about $f/2.5 - f/3.5$ on a high contrast emulsion such as Kodak IIIa-J. The exposure is of such a duration that, after processing, the photographic density of the sky background is 1. The processed emulsion is scanned by an automatic microdensitometer with a pixel size of the scanning beam which is related to the angular structure of the images and the granularity of the emulsion. The detection of the image of the star depends upon its photographic density (the signal) relative to the fluctuation in the density of the background (the noise). Although it is expected that larger Schmidt telescopes will lead to an improvement in detection sensitivity through enhanced signal/noise ratios, the degree of improvement will depend upon the relative importance of the factors which contribute to the size and structure of stellar images. Several of these factors are examined here and the improvement in sensitivity of larger telescopes is determined in terms of the limiting apparent magnitude that will be detected.

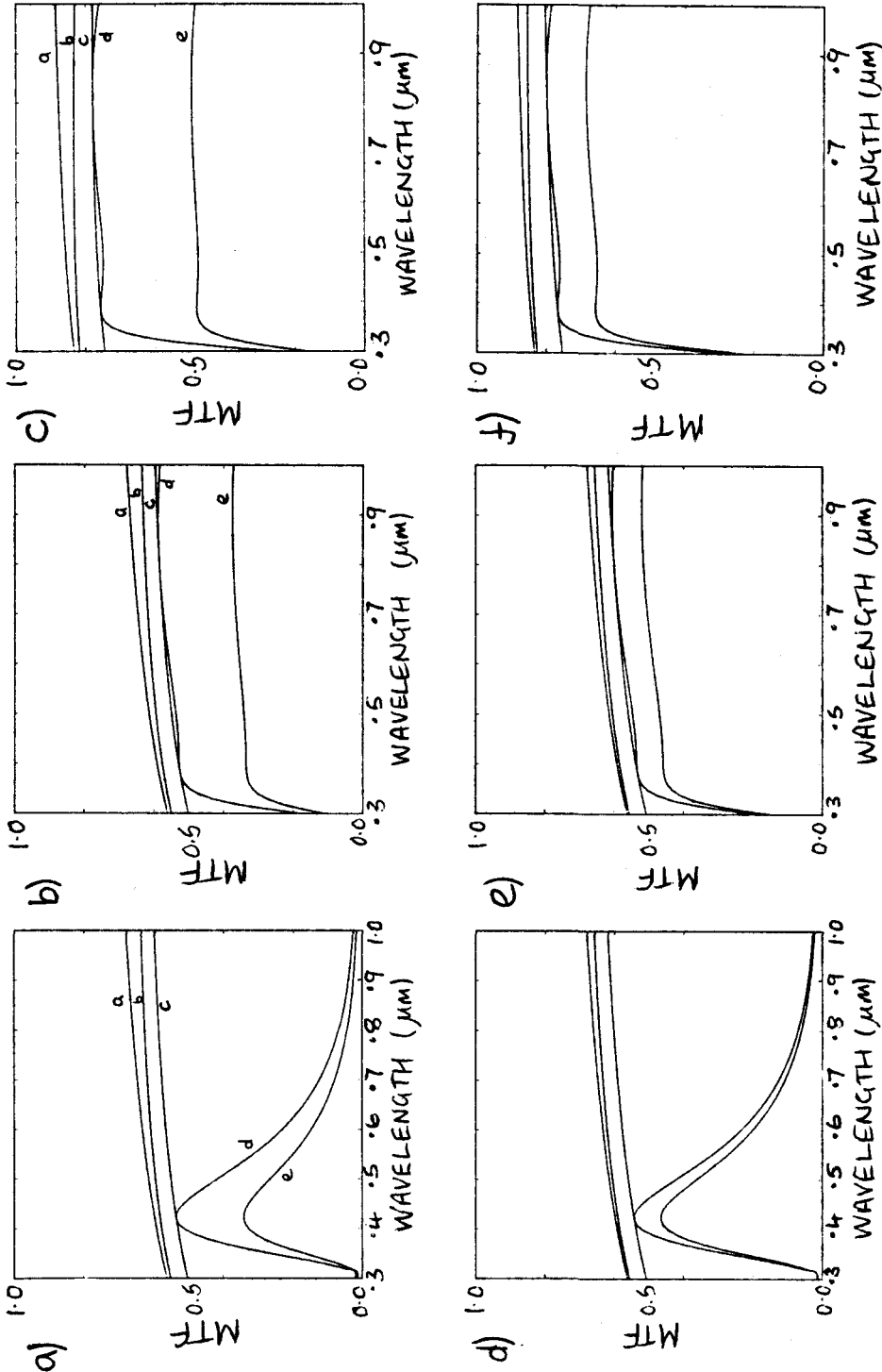


Fig. 1: Modulation values at 0.3 c/arcsec

a) singlet corrector plate b) achromat, $r_0 = 10\text{cm}$ seeing c) achromat, $r_0 = 20\text{cm}$ for 1.24m, $f/2.5$
 d), e), f) for 2.5m, $f/2.5$

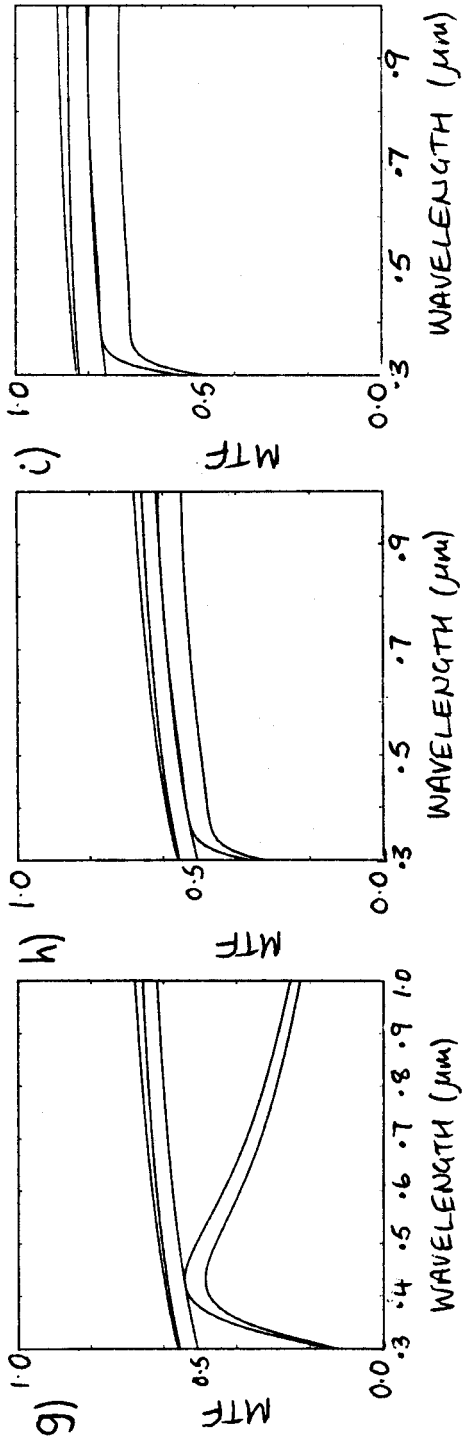


Fig. 1: Modulation values at 0.3 c/arcsec g), h) + i) for 2.5, f/3

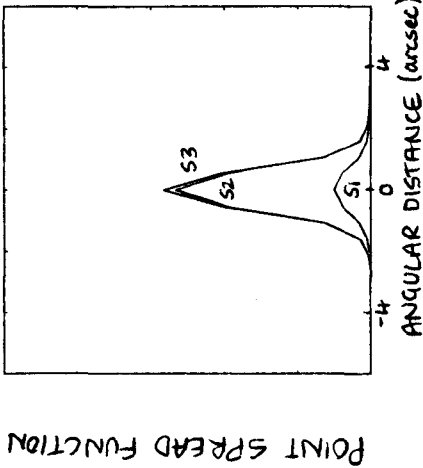


Fig. 2: Point spread function of the star images

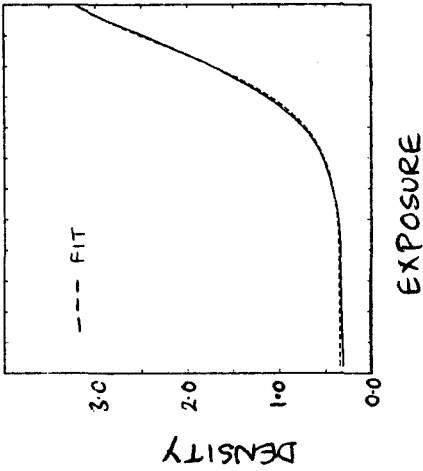


Fig. 3: photographic characteristic of IIIa-J

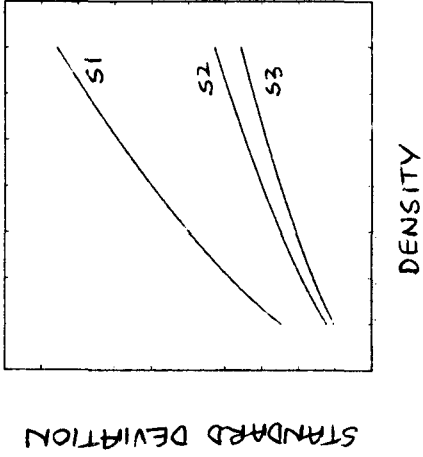


Fig. 4: Furenlid's result.

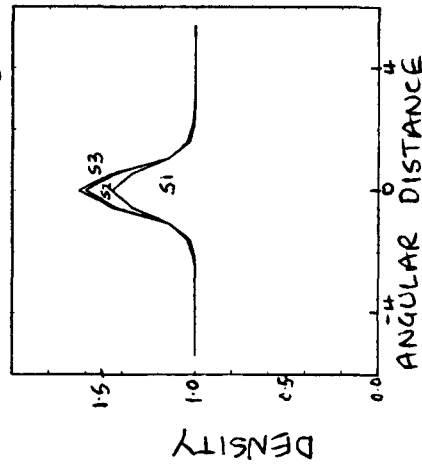


Fig. 5: Stellar density before fluctuations

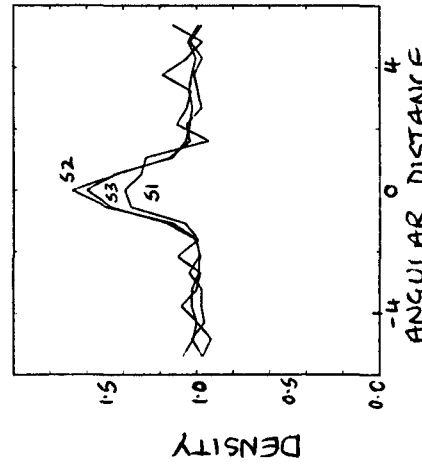


Fig. 6: Stellar density after fluctuations

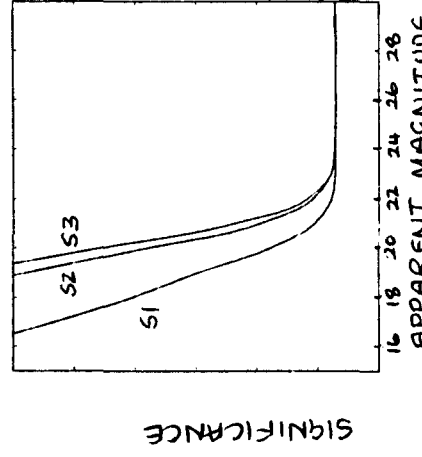


Fig. 7: significance of Stellar density

2. BASIS AND RESULTS OF CALCULATIONS

The steps leading to the formation of the image are that the wavefront reaching the telescope is:

- a) altered in intensity and phase by variations in the refractive index of the atmosphere (the "seeing", represented by $r_0 = 10$ cm for average seeing and $r_0 = 20$ cm for good seeing (ref. 1)),
- b) diffracted at the aperture of the mirror,
- c) changed in phase by the errors in the surfaces. This is akin to very good seeing with $r_0 = 30$ cm,
- d) changed in phase by path length errors in the corrector plate. Two plates have been simulated, a singlet corrected at $\lambda = 0.42 \mu\text{m}$ and an achromat corrected at $\lambda = 0.38$ and $1.0 \mu\text{m}$,
- e) scattered in the recording emulsion which is represented by the Kodak MTF data (ref.2).

A point source provides a wavefront characterised by unit modulations at all spatial frequencies, and each of the above processes is likely to reduce this modulation. The inverse Fourier transform of the modulated distribution leads to an image which necessarily has angular (or linear) breadth. The spatial frequency of each of the response processes has been determined in the usual way and the product of these forms the overall spatial frequency response or modulation transfer function, MTF, from which the image structure or point spread function has been found, PSF.

Representative results of the 5 processes are shown cumulatively in fig. 1 (a-c) for the S1 Schmidt. Modulation values at a single spatial frequency (0.3 c/arc sec) are shown as a function of wavelength. In all the figures the seeing reduces the MTF considerably although this improves slightly at longer wavelengths. Aperture diffraction and surface irregularities are of minor importance whereas the design of the corrector plates is very important. For the singlet (fig. 1a) the MTF is severely reduced away from $\lambda = 0.42 \mu\text{m}$. However the achromat (fig. 1b) is very well corrected and contributes negligibly to the reduction of MTF except in the UV. Finally the effect of scattering in IIIa-J emulsion is seen to be quite important. Indeed in very good seeing (fig. 1c), the emulsion becomes the limiting feature.

The calculations have been repeated for 2 larger Schmidts S2 (in fig. 1d-f) and S3 (in fig. 1g-i). The importance of the focal length is seen here in reducing the residual spherical aberration (c.f. figs. 1a, d, g) and in reducing the effect of the emulsion scatter. So although telescope S2 will collect 4 times as much light as S1 and distribute it over a focal area 4 times larger for sky background, the improvement in MTF with longer focal length will lead to relatively narrower (and hence brighter) star images. This is apparent in fig. 2 where the point spread functions (PSF) of the star images are shown; these have been calculated in average seeing at $\lambda = 0.5 \mu\text{m}$ using the inverse Fourier transform of the MTF.

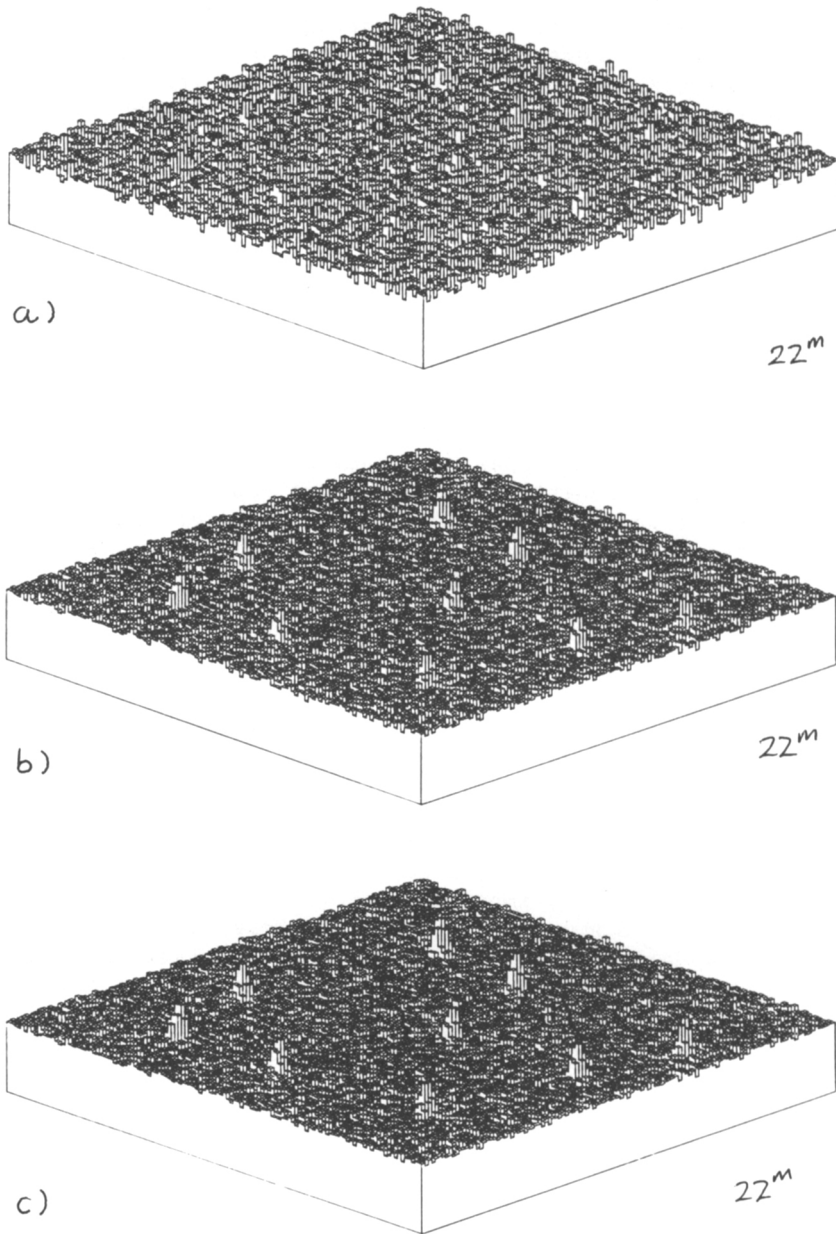


Fig. 8: a) Simulated densitometer trace of star field of Schmidt telescope, S1 (1.24m, $f/2.5$); b) S2 (2.5m, $f/2.5$); c) S3 (2.5m, $f/3$).

However the star image has to be detected by its photographic density relative to that of the sky background. The photographic characteristic of IIIa-J (ref. 2) has been fitted with a physical model (ref. 3) based on fixed grain size ($\sim 0.36 \mu\text{m}^2$) and fixed quantum sensitivity of 2 photons/grain and this is shown in fig. 3. This gives a simple parameterization which is used to determine the exposure to give unit density for the sky background ($22.5^{\text{m}}/\text{arc sec}^2$) and this exposure is used to scale the exposures for stars of a variety of apparent magnitudes and hence to determine their photodensities which are then added to the background sky density.

The simulations are made in 2 dimensions in the photoplate. For S1 the densities were evaluated in pixels of $8 \times 8 \mu\text{m}^2$ where the point spread function of a stellar image covered a 21×21 matrix of such pixels (a total angular size $\sim 10 \times 10 \text{ arc sec}^2$). A single pixel of the sky background covers about 400 developed grains and hence there will be random fluctuations of these from pixel to pixel giving the noise of the system. To simulate this the results of Furenlid (ref.4) have been scaled to pixels of the sizes used here. For the longer focal length telescopes it is the linear size, rather than the angular size, of the image which is increased. To give the same angular resolution the pixel size was increased from $8 \mu\text{m}$ to $16 \mu\text{m}$ for S2 and to $19.2 \mu\text{m}$ for S3. As these larger pixels now cover more grains the relative fluctuations will be reduced. This is seen in fig. 4 where Furenlid's results are shown for the 3 pixel sizes.

The 2-dimensional distributions of photodensity are then randomised by the standard deviation in density fluctuations corresponding to the density and pixel size. One dimensional simulated measurements of density through a star of 22^{m} are shown before fluctuations are added in fig. 5 and after fluctuations in fig. 6 for the 3 designs of telescope.

The limiting magnitude of stars that are just seen has been determined by quantifying a "significance" for the stellar density. For the field of a stellar image of 21×21 pixels the density is made up from starlight (S) and sky background (BG) and randomised according to the grain noise. A further 50 randomised sky background fields have been generated and a significance calculated where

$$\text{Sig} = \sum_{i=1}^{50} \left[(S+BG) - BG_i \right]^2 / 50$$

The significance is shown in fig. 7 for increasing stellar magnitude. When this is such that the star is "lost" in the noise, Sig approaches $\sqrt{2}$. This occurs at about 22^{m} for S1; at about 23^{m} for S2 and at about 23.5 for S3.

To demonstrate this improvement in sensitivity, 9 stars of 22^{m} have been generated in a stellar field of 121×121 pixels for the 3

telescopes. The fields are shown in fig. 8a, b and c.

3. SUMMARY AND CONCLUSIONS

Simulations have been made of the photographic densities of stellar images in 3 Schmidt telescopes (1.24 m, $f/2.5$; 2.5 m, $f/2$; 2.5 m, $f/3$.) The effects on performance of the main factors contributing to image size have been examined. The telescopes are usually limited by seeing but when this is good the 1.24 m, $f/2.5$ telescope would then be limited by the IIIa-J emulsion. This limitation can be removed by doubling the focal length with a corresponding increase in aperture diameter to compensate for loss in light density. When the focal length is increased further (with aperture constant) residual spherical aberration is reduced and the increase in image scale further improves signal/noise but at the expense of increased exposure time for sky limited plates. This is summarised in table 1 where the 3 telescopes were used to expose a background sky density of 1 in $r_0=10$ cm seeing at $\lambda=0.5\mu\text{m}$.

Table 1

	1.24m, $f/2.5$	2.5m, $f/2.5$	2.5m, $f/3$
Exposure	t	t	1.44 t
Signal/noise	S/n	2.93 S/n	4.34 S/n
Limiting sensitivity	22^m	23^m	23.5^m

4. REFERENCES

1. D.L. Fried, 1966, *J. Opt. Soc. Am.* 56, pp (1372-1379)
J.C. Dainty and R.J. Scaddan, 1975, *Mon. Not. R. astron. Soc.* 170, pp(519-532)
2. Kodak publication p-315, 1973
3. J.C. Dainty and R. Shaw, 1974, *Image Science* (Academic Press)
4. I Furenlid, 1978, *Modern Techniques in Astronomical Photography* (ed Hendier and West pp(153-164).